PICOSCALE Vibrometer Performance Specifications

SmarAct | metrology

DISCLAIMER

The information detailed in this document describes the performance of the **PICO**SCALE *Vibrometer* when the device is optimally set-up and under laboratory conditions. Details about the methods used to assess the performances of the **PICO**SCALE *Vibrometer* can be found in Table .

MAIN FUNCTIONAL BLOCKS

SmarAct's **PICO**SCALE *Vibrometer* architecture can be divided into three main blocks, see Figure 1:

- The **optics** block. It includes a stabilized laser source that is current-modulated at 30 MHz, the actual interferometer that contains the necessary optical components to form a Michelson interferometer, and finally a photodiode to measure the interferometric signal.
- The **electronics** block that processes the interferometric signal. It includes various amplifiers and analogue lock-in amplifiers to extract two quadrature signals, here at 60 MHz and 90 MHz.
- The **digital** block that computes the relative displacement between reference and measurement object. It consists of analog-to-digital converters and appropriate routines that can stream data to a computer via USB or Ethernet connections.

  In *Local Analysis*, the interferometric laser beam is locked to a given position and the displacement signal is recorded. This signal can be Fourier transformed to reveal the characteristic of the vibrations.

  In *Modal Analysis*, the interferometric laser beam is raster-scanned over an excited measurement object. The relative displacement is processed on-the-fly using a digital dual-phase lock-in amplifier that extracts both phase and amplitude information.

This document aims to thoroughly investigates the limitations of the **PICO**SCALE *Vibrometer* and analyze the impact of each block with respect to the resolution, accuracy and precision of the device.

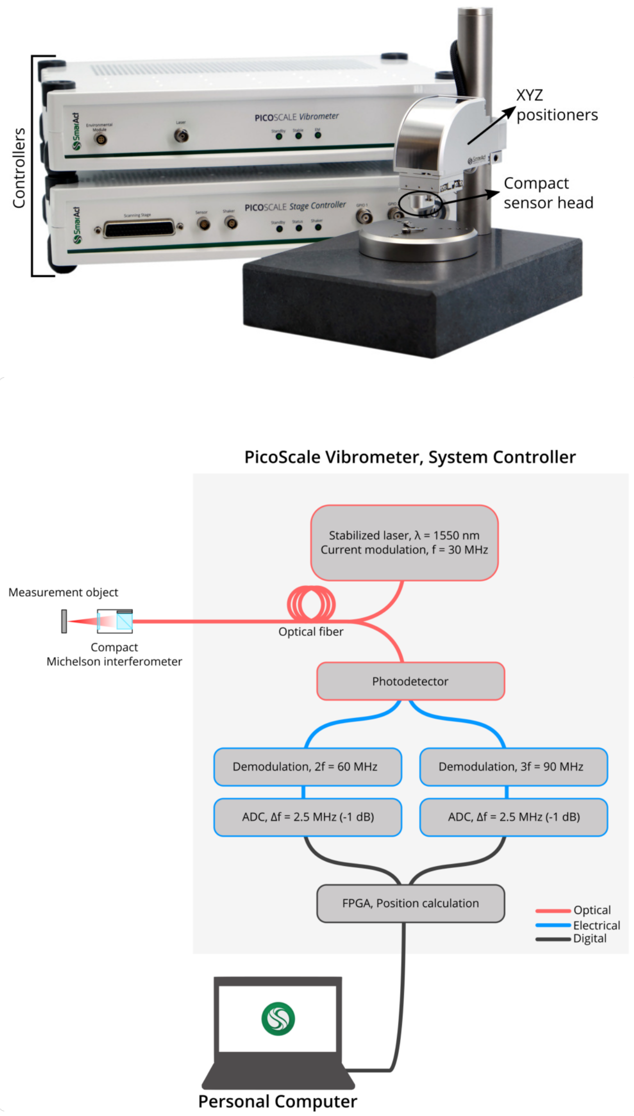

Figure 1. *Functional blocks of SmarAct's **PICO**SCALE Vibrometer.*

DEFINITIONS

The notations used in this document are displayed in Table 1:

Table 1. *Notations and definitions*

Symbol	Definition
r	Imaging resolution
λ_{1550nm}	Wavelength 1550 nm
NA	Objective numerical aperture
n_i	Refractive index of medium i
W	Total rms noise
ASD	Amplitude Spectral Density
Δf	Bandwidth, frequency range
$\overline{W}$	Mean noise level
THD	Total harmonic distortion
A_i	Amplitude at the harmonic i
S	Maximum spurious signal
R_R	Reflectivity ratio
A	Amplitude
f_s	Frame rate
f	Frequency
sdr	Smallest digital representation, 1 pm
I	Intensity of the interferometric signal
τ	Time response
R	Decimator factor
ϵ	Error
Δ_J	Measurement jitter, <40 ns
Θ	Tilt between object and sensor

Relative reflectivity
"*The quadrature signals form a Lissajous circle, whose radius is proportional to the reflectivity of the sample. The relative reflectivity is the current radius divided by the radius achieved with a perfectly reflecting target.*"

Signal quality
"*The signal quality is an internal data type. It is a dimensionless quantity proportional to the current of the photodiode.*"

Lateral resolution
"*The lateral resolution is defined as the minimum distance to adequately distinguish two closely spaced points.*"

$$r_{lateral}[m] = 0.44 \cdot \lambda_{1550nm} \cdot NA^{-1} \quad (1)$$

Axial resolution
"*The axial resolution represents the sensitivity to points reflectors along the propagation of the laser beam.*"

$$r_{axial}[m] = 1.4 \cdot \lambda_{1550nm} \cdot NA^{-2} \quad (2)$$

Working frequency range
"*The working frequency range is the usable vibration frequency range of the vibrometer. Outside this frequency range, the amplitude of vibration will be significantly damped and phase errors will be introduced.*"

Maximum measurement amplitude
"*The maximum measurement amplitude consists of the maximum detectable movement of the measurement object with respect to the sensor over the working frequency range.*"

Total rms and mean noise level
"*The total rms noise level corresponds to the minimum resolvable step in time domain while the mean noise level defines the detection limit of the **PICO**SCALE Vibrometer.*"

$$W[m_{rms}] = \sqrt{\sum (ASD \cdot \Delta f)^2}; \qquad \overline{W}[m_{rms}/\sqrt{Hz}] = \overline{ASD} \quad (3)$$

Total harmonic distortions
"*The total harmonic distortion is defined as the unwanted spectral components at the harmonics of the fundamental frequency.*"

$$THD[\%] = \sqrt{\sum_{i=2}^{i=\infty} A_i^2 \cdot A_0^{-1}} \cdot 100, \quad (4)$$

Maximum spurious signal
"*The maximum spurious signal is defined as the highest absolute level of unwanted spectral components. Harmonic distortions are not considered.*"

$$S[m_{rms}/\sqrt{Hz}] = max(ASD) \quad (5)$$

Reflectivity ratio
The reflectivity ratio between two measurement points is calculated as followed:

$$R_R = R_{max} \cdot R_{min}^{-1} \quad (6)$$

with R_{max} and R_{min} being the maximum and minimum reflectivity between the points respectively.

MICROSCOPY

General

Table 2 summarizes the requirements to allow microscopy measurement.

Table 2. *Requirements*

Specification	Values
Measurement object features XY	$\geqslant r_{lateral}$
Measurement object reflectivity	$>$ 3.5%, λ_{1550nm}
Relative reflectivity	$\geqslant$ 5%
Signal quality	$\geqslant$ 50

Lateral resolution

Table 3 specifies the different lateral resolutions.

Table 3. *Lateral resolution for different sensor heads.*

Sensor Head	$r_{lateral}$ [µm]
F03 NA0.15	6
F03 NA0.25	4
F03 NA0.50	2

During imaging, the smallest pixel size is also limited by the positioning system which can trigger the data acquisition every 1 µm.

Axial resolution

Table 4 specifies the different axial resolution.

Table 4. *Axial resolution for different sensor heads.*

Sensor Head	r_{axial} [µm]
F03 NA0.15	95
F03 NA0.25	35
F03 NA0.50	7

Calibration factor

Periodic non-linearity

Microscopy information is retrieved from the relative reflectivity. Prior calculation of the relative reflectivity, internal routines ensure that the quadrature signals are normalized and properly in quadrature. The output relative reflectivity signal suffers however from periodic non-linear errors originating from erroneous corrections and presence of multipath interferences. These errors depend on the devices, the measurement objects and the environmental conditions.

In case of microscopy measurement, the periodic non-linear errors result in a periodic pattern within the microscopy image of period $\lambda_{1550nm}/2$ and $\lambda_{1550nm}/4$. The relative reflectivity fluctuates up to 5%.

TOPOGRAPHY

General

Table 5 summarizes the requirements to allow topography measurement.

Table 5. *Requirements*

Specification	Values
Measurement object features XY	$\geqslant r_{lateral}$
Measurement object features Z	$\leqslant r_{axial}$
Measurement object reflectivity	$>$ 3.5%, λ_{1550nm}
Relative reflectivity	$\geqslant$ 5%
Signal quality	$\geqslant$ 50

To unambiguously estimate the measurement object height, the height between two neighboring pixels of the topography image should be below $\lambda_{1550nm}/2$, or $\approx$775 nm.

Resolution and accuracy

The resolution of the topography measurement is 50 nm and the accuracy is 250 nm.

OUT-OF-PLANE VIBRATIONS

General

Table 6 summarizes the requirements to allow out-of-plane vibration measurement.

Table 6. *Requirements*

Specification	Values
Measurement object features XY	$\geqslant r_{lateral}$
Measurement object reflectivity	$>$ 3.5%, λ_{1550nm}
Relative reflectivity	$\geqslant$ 5%
Signal quality	$\geqslant$ 50

Table 7 summarizes the different data sources available when measuring out-of-plane vibrations during *Local Analysis*.

Table 7. *Available data sources*

Data sources	f_s [MHz]
Displacement	$\leqslant$ 10
Sensor	$\leqslant$ 10

All data sources can be displayed and saved in either the time domain (raw data, unprocessed) or in the frequency domain (post-processed data).

Working frequency range

The working frequency range is summarized in Table 8.

Table 8. *Working frequency range*

Measurement	Δf [Hz]
Local Analysis	[DC : 2.5M]
Modal Analysis	[50 : 2.5M]

In *Local Analysis*, the working frequency range is limited by the analogue lock-in amplifiers that extracts both quadrature signals. The cutoff frequency of the low-pass filters is 2.5 MHz at $-1\,dB$.
In *Modal Analysis*, the working frequency range is further reduced because of the dual-phase lock-in amplifier. Prior demodulation, the relative displacement signal is high-pass filtered. This high-pass filter has a corner frequency at $-3dB$ of 50 Hz.

Maximum measurement amplitude

In *Modal Analysis*, the maximum measurement amplitude is given by:

$$A_{max}[m] = \frac{\lambda_{1550nm}}{4} \cdot \frac{f_s}{2\pi \cdot f} \tag{7}$$

In *Local Analysis*, it is further limited by data compression:

$$A_{max}[m] = 2^{16} \cdot sdr \cdot \frac{f_s}{2\pi \cdot f} \tag{8}$$

Both maximum measurement amplitudes are shown in Table 9.

Table 9. *Maximum measurement amplitude at 10 MHz.*

f [Hz]	Local A_{max} [m]	Modal A_{max} [m]
1	104m	617m
10	10m	62m
100	1m	6m
1k	104μ	617μ
10k	10μ	62μ
100k	1μ	6μ
1M	104n	617n

The **PICO**SCALE *Vibrometer* uses confocal optics which further reduces the maximum measurement amplitude to the objective axial resolution.

Total rms and mean noise level

Both noise levels are not constant over the working frequency range and are influenced by the signal quality, relative reflectivity, calibration factors as well as environmental noise. They are thus defined over frequency bands. During imaging, the moving positioning system also contributes to the noise.
The total rms and mean noise levels are summarized in Table 10 and Table 11.
Electronics noise dominates in the frequency bands above 100 kHz. Here, the total rms noise level and mean noise level can fluctuate by 50%.
The noise levels depend strongly on the signal quality of the interferometric signal. They are approximately proportional to $-\log(signalquality)$ if the signal quality is below 100.

Table 10. *Static: total rms and mean noise level*

Band [Hz]	W [pm_{rms}]	$\overline{W}$ [$pm_{rms}/\sqrt{Hz}$]
1 - 10	150	40
10 - 100	300	30
100 - 1k	100	4
1k - 10k	175	2
10k - 100k	175	0.6
100k - 1M	600 (900)	0.6 (0.9)
1M - 5M	400 (600)	0.2 (0.4)
Total	**839** (1164)	n.a

Table 11. *Dynamic: total rms and mean noise level*

Band [Hz]	W [pm$_{rms}$]	$\overline{W}$ [pm$_{rms}/\sqrt{Hz}$]
1 - 10	25000	8000
10 - 100	7500	750
100 - 1k	4000	150
1k - 10k	3000	30
10k - 100k	1500	5
100k - 1M	600 (900)	0.6 (0.9)
1M - 5M	400 (600)	0.2 (0.4)
Total	**26627** (26640)	n.a

Total harmonic distortions
The total harmonic distortion is less than 2.5%. The corresponding maximum relative level is −70 dB.

Maximum spurious signal
The maximum spurious signals, given for each frequency band, are displayed in Table 12.

Table 12. *Maximum spurious signal*

Band [Hz]	S [pm$_{rms}/\sqrt{Hz}$]
1 - 10	75
10 - 100	100
100 - 1k	20
1k - 10k	2.25
10k - 100k	2.5
100k - 1M	10
1M - 5M	0.75

Dual-phase lock-in amplifier bandwidth and time response
In *Modal Analysis*, the relative displacement signal serves as input for the dual-phase lock-in amplifier. Table 13 summarizes the dual-phase lock-in amplifier performances at 10 MHz.

Table 13. *Specifications at $F_s = 10\,MHz$*

Configuration	Δf_{10MHz} [kHz]	τ_{10MHz} [µs]
Fine	16	43.2
Narrow	32	21.6
Normal	64	10.8
Wide	128	5.4

Both bandwidth and time response are affected by the downsampling rate of the decimator prior demodulation according to:

$$\Delta f_{fs} = \Delta f_{10MHz} \cdot R^{-1}, \quad \tau_{fs} = \tau_{10MHz} \cdot R \tag{9}$$

Calibration factors
Wavelength uncertainty
The relative displacement, thus the amplitude of vibration, measured by a michelson-based vibrometer is directly proportional to the wavelength of the laser. The **PICO**SCALE *Vibrometer* uses a laser source which is stabilized to an absorption cell which is traceable to NIST standards. The error on the wavelength is given by $\lambda \cdot 10^{-6}$. The effect on the measurement is then negligible within the measurement range.

Periodic non-linearity
The relative displacement signal suffers from periodic non-linear errors originating from erroneous corrections and presence of multipath interferences. These errors depend on the devices, the measurement objects and the environmental conditions. It is then only possible to provide a worst-case scenario which is taken as the limitation of the **PICO**SCALE *Vibrometer*. The worst-case scenario is a 8 nm-induced periodic non-linear error on the relative displacement signal that can sometimes occur if the system is not properly adjusted at focus. In most cases, it is much less than 5 nm. Under these conditions, the induced error on the amplitude of vibration is shown in Table 14.

Table 14. *Amplitude error from periodic non-linearity.*

Range [m]	$\epsilon_{amplitude}$ [%]
1p - 10p	6
10p - 100p	6
100p - 1n	6
1n - 10n	6
10n - 100n	6
100n - 1µ	1
1µ - 10µ	0.1
10µ - 100µ	0.02

Compensator
In *Modal Analysis*, the amplitude of vibration is extracted using a digital dual-phase lock-in amplifier. This digital component has been calibrated to compensated for induced damping. The amplitude error is less than 0.025% within the working frequency range.

Digital signal output jitter
In *Local Analysis*, it is possible to average multiple time series in a row. It exists however an intrinsic measurement jitter of less than 40 ns that will affect the

measurement of the phase and amplitude of the vibrations:

$$\epsilon_{phase}[\%] = \Delta_J \cdot f \cdot 100, \\ \epsilon_{amplitude}[\%] = (1 - \cos(\Delta_J \cdot \pi \cdot f)) \cdot 100 \quad (10)$$

Both errors are shows in Table 15.

Table 15. *Error from the digital signal output jitter.*

f [Hz]	$\epsilon_{amplitude}[\%]$	$\epsilon_{amplitude}[\%]$
1	790f	4μ
10	79p	40μ
100	7.9n	400μ
1k	790n	4m
10k	79μ	40m
100k	7.9m	400m
1M	789m	4
5M	19	20

In the frequency domain, the amplitude of vibration remains unaffected because of the incoherent averaging.

High-aperture effects

The **PICO**SCALE *Vibrometer* uses confocal optics which is sensitive to the Gouy phase shift. The impact of such phase shift depends on the sensor head in used but overall, the error on the amplitude of vibration will be less than 3.5% up to 100 μm vibration amplitude, see Table 16.

Table 16. *Amplitude error from high-aperture effects.*

Sensor Head	$\epsilon_{amplitude,max}$ [%]
F03 NA0.15	0.25
F03 NA0.25	0.80
F03 NA0.50	3.50

Influence of the medium

The **PICO**SCALE *Vibrometer* assumes that the interferometric laser beam travels through a medium of refractive index equals to 1. If the measurement object is fully contained within a medium of different index, the amplitude of vibration will be affected such that:

$$A_{true}[m] = A_{measured} \cdot n_i^{-1} \quad (11)$$

In air, the refractive index is 1.00027. The error is then negligible.

Influence of the measurement object tilt

The existence of tilt between measurement object and optical path affects the measurement of the true amplitude such that:

$$A_{true}[m] = A_{measured} \cdot \cos(\Theta) \quad (12)$$

The worst-case scenario occurs if the tilt equals the angular range of the sensor heads, see Table 17.

Table 17. *Amplitude error from measurement object tilt.*

Sensor Head	$\epsilon_{amplitude,max}$ [%]
F03 NA0.15	0.30
F03 NA0.25	0.60
F03 NA0.50	3.00

IN-PLANE VIBRATIONS

General

Table 18 summarizes the requirements to allow in-plane vibration measurement.

Table 18. *Requirements*

Specification	Values
Measurement object features XY	$\geqslant r_{lateral}$
Measurement object reflectivity	$>$ 3.5%, λ_{1550nm}
Relative reflectivity	$\geqslant$ 5%
Signal quality	$\geqslant$ 50
Reflectivity ratio	$\gg$ 1

Table 19 summarizes the different data sources available when measuring in-plane vibrations during *Local Analysis*.

Table 19. *Available data sources*

Data sources	f_s [MHz]
Relative reflection	$\leqslant$ 5
Sensor	$\leqslant$ 10

All data sources can be displayed and saved in either the time domain (raw data, unprocessed) or in the frequency domain (post-processed data).

Working frequency range

In *Stroboscopic Analysis*, the working frequency range is limited by the analogue lock-in amplifiers that extracts both quadrature signals. The cutoff frequency of the low-pass filters is 2.5 MHz at −1 dB.
In *Knife-edge Analysis*, the working frequency range is futher reduced because of the dual-phase lock-in amplifier. Prior demodulation, the relative reflection signal is high-pass filtered. This high-pass filter has a corner frequency at −3 dB of 50 Hz.
The working frequency range for each analysis is displayed in Table 20.

Table 20. *Working frequency range*

Measurement	Δf [Hz]
Stroboscopic Analysis	[DC : 2.5M]
Knife-edge Analysis	[50 : 2.5M]

Maximum measurement amplitude

In *Modal Analysis*, the maximum measurement amplitude is given by:

$$A_{max}[m] = \frac{\lambda_{1550nm}}{4} \cdot \frac{f_s}{2\pi \cdot f} \qquad (13)$$

In *Local Analysis*, it is further limited by data compression:

$$A_{max}[m] = 2^{16} \cdot sdr \cdot \frac{f_s}{2\pi \cdot f} \qquad (14)$$

Both maximum measurement amplitudes are shown in Table 21.

Table 21. *Maximum measurement amplitude at 5 MHz.*

f [Hz]	Local A_{max} [m]	Modal A_{max} [m]
1	51m	308m
10	5m	31m
100	512µ	3m
1k	51µ	308µ
10k	5µ	31µ
100k	512n	3µ
1M	51n	308n

Total rms and mean noise level

Both noise levels are not constant over the working frequency range and are influenced by the signal quality, relative reflectivity, calibration factors as well as environmental noise. They are thus defined over frequency bands. During imaging, the moving positioning system also contributes to the noise.
The total rms and mean noise levels are summarized in Table 22 and Table 23.

Electronics noise dominates in the frequency bands above 100 kHz. Here, the total rms noise level can fluctuate by 50%.
The noise levels depend strongly on the signal quality of the interferometric signal. They are approximately proportional to $-\log(signalquality)$ if the signal quality is below 100.

Table 22. *Static: total rms and mean noise level*

Band [Hz]	W [pm_{rms}]	$\overline{W}$ [$pm_{rms}/\sqrt{Hz}$]
1 - 10	600	200
10 - 100	300	40
100 - 1k	400	15
1k - 10k	1000	10
10k - 100k	1000	4
100k - 1M	3000 (4500)	4
1M - 2.5M	2500 (3750)	3
Total	**4226** (6076)	n.a

Table 23. *Dynamic: total rms and mean noise level*

Band [Hz]	W [pm_{rms}]	$\overline{W}$ [$pm_{rms}/\sqrt{Hz}$]
1 - 10	1500	455
10 - 100	600	55
100 - 1k	3000	90
1k - 10k	2500	25
10k - 100k	1000	4
100k - 1M	3000 (4500)	4
1M - 2.5M	2500 (3750)	3
Total	**5840** (7292)	n.a

Harmonic distortions
The total harmonic distortion is less than 7.5%. The corresponding maximum relative level is −50 dB.

Maximum spurious signal
The maximum spurious signals, given for each frequency band, are displayed in Table 24.

Table 24. *Static: Maximum spurious signal*

Band [Hz]	S [$pm_{rms}/\sqrt{Hz}$]
1 - 10	400
10 - 100	100
100 - 1k	20
1k - 10k	20
10k - 100k	15
100k - 1M	150
1M - 2.5M	10

Dual-phase lock-in amplifier bandwidth and time response
In *Knife-edge Analysis*, the relative reflection signal serves as input signal for the dual-phase lock-in amplifier.
Table 25 summarizes the dual-phase lock-in amplifier performances at 10 MHz.

Table 25. *Specifications at* $F_s = 10\,MHz$

Configuration	Δf_{10MHz} **[kHz]**	τ_{10MHz} **[µs]**
Fine	16	43.2
Narrow	32	21.6
Normal	64	10.8
Wide	128	5.4

Both bandwidth and time response are affected by the downsampling rate of the decimator prior demodulation according to:

$$\Delta f_{fs} = \Delta f_{10MHz} \cdot R^{-1}, \quad \tau_{fs} = \tau_{10MHz} \cdot R \tag{15}$$

Calibration factors
Positioning system
The in-plane vibration amplitude is directly proportional to the pixel size. It is then dependent on the positioning system accuracy. The error on the lateral amplitude for a CLS-3232 is less than 1%.
However, the calculation of the lateral amplitude depends also on the post-processing of the sequential images. The stated accuracy for the template matching algorithm used is 15%.

Digital signal output jitter
In *Local Analysis*, it is possible to average multiple time series in a row. It exists however an intrinsic measurement jitter of less than 40 ns that will affect the measurement of the phase and amplitude of the vibrations:

$$\epsilon_{phase}[\%] = \Delta_J \cdot f \cdot 100, \quad \epsilon_{amplitude}[\%] = (1 - \cos(\Delta_J \cdot \pi \cdot f)) \cdot 100 \tag{16}$$

Both errors are shows in Table 26.

Table 26. *Error from the digital signal output jitter.*

f [Hz]	$\epsilon_{amplitude}[\%]$	$\epsilon_{amplitude}[\%]$
1	790f	4µ
10	79p	40µ
100	7.9n	400µ
1k	790n	4m
10k	79µ	40m
100k	7.9m	400m
1M	789m	4
2.5M	4.9	10

In the frequency domain, the amplitude of vibration remains unaffected because of the incoherent averaging.

MEASUREMENT METHODS

General

The components used are listed below:

Table 27. *Components*

Components	Product name
Support	Thorlabs POC001
Hood	Accurion Nano20
System controller	SmarAct PV-CTRL-V1.0-TAB
Stage controller	SmarAct PV-STG-V1.0-TAB
XYZ stage controller	SmarAct PV-XYZ-V1.0
Sensor Head	SmarAct PV-SH-F03, NA0.15

The environmental conditions are listed below:

Table 28. *Measurement conditions*

Parameters	Values
Temperature	21 °C
Humidity	40 %RH
Pressure	1022 hPa

Working frequency range

The working frequency range based on the dual-phase lock-in amplifier high pass filter (in *Modal Analysis*) is *i*) defined when designing the filter and *ii*) controlled using synthetic signals. The synthetic signals are generated using the signal generator of the **PICO**SCALE *Vibrometer*.
To measure the bandwidth, the dual-phase lock-in amplifier is locked to 1 kHz. The synthetic signal corresponds to a linear chirp with frequency ramping from 0.1 kHz to 10 kHz over 1 s. The digital signal serves as input signal of the dual-phase lock-in amplifier. The resulting amplitude signal is post-analyzed to retrieve the bandwidth at −3 dB.

Total rms and mean noise level

The interferometric laser beam is positioned at focus on the measurement object (ME1-P01, Thorlabs).
For the complete bandwidth, two measurements were performed:

1. Frequency band [1-1k[Hz: sampling rate set at 312.5 kHz (correspondingly, an anti-aliasing filter is applied) and time series duration set to 1 s. 100 averages are recorded. Each time series is fourier transformed using a rectangular window. The resulting spectra are averaged.

2. Frequency band [1k-10M]Hz: sampling rate set at 10 MHz and time series duration set to 0.1 s. 100 averages are recorded. Each time series is fourier transformed using a rectangular window. The resulting spectra are averaged.

The final averaged spectra are then post-analyzed. The analysis consists in binning the spectra according to the frequency band and calculating the appropriate parameters.

Dynamic

The measurement object is fixed on the fast axis of an additional PV-XYZ-V1.0 which is put in movement. The additional PV-XYZ-V1.0 is configured as follow:

Table 29. *Movement specifications*

Components	Name
Velocity	0.1 m s^{-1}
Acceleration	0.1 m s^{-2}
Trajectory	Triangular
Travelling range	100 µm

Harmonics distortion

The measurement object is actively actuated and the corresponding ASD is recorded. The post-analysis of the ASD consists in finding the amplitude at each harmonics within the full bandwidth.

Out-of-plane vibration

The shaker stage is actuated at 1 kHz with maximum amplitude (5 V to 10 V). 25 time series of 2 s duration are recorded at 321.5 kHz (correspondingly, an anti-aliasing filter is applied). Each time series is fourier transformed using a rectangular window. The resulting spectra are averaged.

Table 30. *Out-of-plane: measurement object and actuation.*

Measurement Object	Actuation
ME-P01 (Thorlabs)	SmarAct PV-SHK-V1.0

In-plane vibration

The measurement object is excited using the shaker output signal (5 V to 10 V) with maximum amplitude. The actuation frequency is 2.598 kHz. 25 time series of 2 s duration are recorded at 321.5 kHz (correspondingly, an anti-aliasing filter is applied). Each time series is fourier transformed using a rectangular window. The resulting spectra are averaged.

Table 31. *In-plane: measurement object and actuation.*

Measurement Object	Actuation
FT-G gripper (Femto Tools)	Direct

Maximum spurious signal
The maximum spurious signal is measured similarly than the total rms and mean noise level.

Dual-phase lock-in amplifier bandwidth and time response
The bandwidth and the time response of the dual-phase lock-in amplifier are *i*) defined when designing the filters and *ii*) measured using synthetic signals. The synthetic signals are generated using the signal generator of the **PICO**SCALE *Vibrometer*.
To measure the bandwidth, the dual-phase lock-in amplifier is locked to 1 kHz. The synthetic signal corresponds to a linear chirp with frequency ramping from 0.1 kHz to 10 kHz over 1 s. The synthetic signal corresponds to a linear chirp with frequency ramping from 0.1 kHz to 10 kHz over 1 s. The digital signal serves as input signal of the dual-phase lock-in amplifier. The resulting amplitude signal is post-analyzed to retrieve the bandwidth at −3 dB.
To measure the time response, the dual-phase lock-in amplifier is locked to 1 kHz. A synthetic sine with 1 kHz oscillation frequency is generated using the internal signal generator of the **PICO**SCALE *Vibrometer*. The amplitude is abruptly changed from 1 to 0. The amplitude signal measured by the dual-phase lock-in amplifier is analyzed. The time to record the change of amplitude is used as time response.

Calibration factors
Periodic non-linearity
Multiple periodic non-linear errors are measured after changing the measurement conditions. The worst-case scenario is used as the basis for the subsequent analysis.
The effect of the periodic non-linear errors is simulated while mimicking the experimental worst-case scenario. The simulation consists in measuring the amplitude error of a specific amplitude of vibration along 36 phase points equidistant by 10°. The maximum error for the specific amplitude of vibration is taken. The simulation is repeated with amplitude of vibration ranging from 100 fm to 100 µm.

Lock-in amplifier compensator
The error on the amplitude from the dual-phase lock-in amplifier is measured using synthetic signals. The synthetic signals are generated using the internal signal generator of the **PICO**SCALE *Vibrometer*. The original amplitude is compared with the amplitude as measured by the dual-phase lock-in amplifier.

Digital signal output jitter
The intrinsic measurement jitter is measured experimentally. A measurement trigger is sent out from *GPIO2* and read in via the *Sensor* input using a standard BNC cable (1 m length). The *Sensor* signal is streamed at 10 MHz for a duration of 100 µs. 50 time series are recorded and post-analyzed.
The post-analysis consists in interpolating the time series derivative by a factor of 10. The temporal position of the derivative minima is then used as comparison marker for each time series. The standard deviation of the temporal positions of the derivative minima is taken as the intrinsic jitter of the measurement.

High-aperture effects
The effect of a high-aperture objective is simulated. The simulation consists in computing the amplitude of vibration without and with the Gouy phase shift:

$$\alpha_{Gouy} = \arctan\left(\frac{z \cdot \lambda_{1550nm}}{\pi \cdot r_{lateral}^2}\right)$$

with z the distance from focus. The distance from focus is modulated to mimic a vibration.
The simulation is repeated with multiple modulation amplitude ranging from 100 fm to 100 µm.

In-plane vibration: conversion from noise level in % to m
The direct noise level measurement while measuring in-plane vibrations is given in the unit of the relative reflection signal, thus in %. The conversion to m is given by:

$$W[m_{rms}] \approx W[\%_{rms}] \cdot r_{lateral} \cdot 0.01 \qquad (17)$$

Contact

Germany

SmarAct Metrology GmbH & Co. KG

Rohdenweg 4
D-26135 Oldenburg
Germany

T: +49 (0) 441 - 800879-0
Email: metrology@smaract.com
www.smaract.com

France

SmarAct GmbH

Schuette-Lanz-Strasse 9
26135 Oldenburg
Germany

T: +49 441 - 800 879 956
Email: info-fr@smaract.com
www.smaract.com

USA

SmarAct Inc.

2140 Shattuck Ave. Suite 302
Berkeley, CA 94704
United States of America

T: +1 415 - 766 9006
Email: info-us@smaract.com
www.smaract.com

China

Dynasense Photonics

6 Taiping Street
Xi Cheng District,
Beijing, China

T: +86 10 - 835 038 53
Email: info@dyna-sense.com
www.dyna-sense.com

Natsu Precision Tech

Room 515, Floor 5, Building 7,
No.18 East Qinghe Anning
Zhuang Road,
Haidian District
Beijing, China

T: +86 18 - 616 715 058
Email: chenye@nano-stage.com
www.nano-stage.com

Shanghai Kingway Optech Co.Ltd

Room 1212, T1 Building
Zhonggeng Global Creative Center
Lane 166, Yuhong Road
Minhang District
Shanghai, China

Tel: +86 21 - 548 469 66
Email: sales@kingway-optech.com
www.kingway-optech.com

Japan

Physix Technology Inc.

Ichikawa-Business-Plaza
4-2-5 Minami-yawata,
Ichikawa-shi
272-0023 Chiba
Japan

T/F: +81 47 - 370 86 00
Email: info-jp@smaract.com
www.physix-tech.com

South Korea

SEUM Tronics

1109, 1, Gasan digital 1-ro
Geumcheon-gu
Seoul, 08594,
Korea

T: +82 2 - 868 10 02
Email: info-kr@smaract.com
www.seumtronics.com

Israel

Optics & Motion Ltd.

P.O.Box 6172
46150 Herzeliya
Israel

T: +972 9 - 950 60 74
Email: info-il@smaract.com
www.opticsmotion.com

SmarAct Metrology GmbH & Co. KG develops sophisticated equipment to serve high accuracy positioning and metrology applications in research and industry within fields such as optics, semiconductors and life sciences. Our broad product portfolio – from miniaturized interferometers and optical encoders for displacement measurements to powerful electrical nanoprobers for the characterization of smallest semiconductor technology nodes – is completed by turnkey scanning microscopes which can be used in vacuum, cryogenic or other harsh environments.
We maintain the complete production in house for a high level of customization so that we can always provide you the optimal individual or OEM solution. We also offer feasibility studies, measurement services and comprehensive support to accompany you along your projects.

Headquarters

SmarAct GmbH

Schuette-Lanz-Strasse 9
26135 Oldenburg
Germany

T: +49 441 - 800 879 0
Email: info-de@smaract.com
www.smaract.com

USA

SmarAct Inc.

2140 Shattuck Ave. Suite 302
Berkeley, CA 94704
United States of America

T: +1 415 - 766 9006
Email: info-us@smaract.com
www.smaract.com